Instrument Science Report COS 2024-05(v1)

COS LP6 Exploratory Resolution Program

Kate Rowlands[1,2], Bethan L. James[1,2], Rachel Plesha[2], Travis C. Fischer[1,2], Christian Johnson[2], Marc Rafelski[2], Julia Roman-Duval[2], David Sahnow[2]

[1] AURA for ESA, Space Telescope Science Institute, Baltimore, MD
[2] Space Telescope Science Institute, Baltimore, MD

28 March 2024

ABSTRACT

In preparation for the enabling of Lifetime Position 6 (LP6) and future lifetime positions, we measured the COS FUV spectral resolution at +7", +9" and +11" above LP1 on the detector. We performed observations of the star AzV80 using cenwaves G130M/1222 and G160M/1577. Our analysis shows a decrease in the resolution from $R \sim 9000 - 13000$ *at +7",* $R \sim 8000 - 12000$ *at +9", to* $R \sim 7000 - 10000$ *at +11', with the spectral resolution being on average 30% lower at +7" than that at LP2 (+3.5" above LP1). The decrease in resolution motivated the placement of LP6 as close as possible to LP5, +6.5" above LP1 both to maintain high resolution at LP6, and allow a future LP above LP6 with sufficient resolution for most science cases.*

Contents

Operated by the Association of Universities for Research in Astronomy, Inc., for the National Aeronautics and Space Administration.

1. Introduction

The COS FUV detector experiences gain sag at the positions of science operations. To maintain the quality of COS science data, periodic lifetime position (LP) moves are required and have taken place since 2012. During the LP6 exploratory investigation, while G160M was at LP4, we had planned to move G130M/1222 to LP6 in addition to the G160M cenwaves. Given the choice to place LP6 close to LP5, there was insufficient space to put 1222 at LP6 since the continuum trace would overlap heavily with LP5 (James et al. 2023a). Since the 1222 still had significant life remaining at LP4, it was decided to keep this cenwave at LP4 for the time being. To prolong the lifetime of LP4 (where overheads are lower), the COS team enabled operations at LP6 as the default position for G160M exposures before the end of life of LP4. We present results from Hubble Space Telescope (HST) Program 16495, designed to measure the spectral resolution at +7", +9" and +11" relative to LP1 (XD=+3.5", XD=+5.5" and XD=+7.5" from LP2, where XD is cross-dispersion position), encompassing the potential LP6 detector positions. The analysis provided here was part of the exploratory phase for LP6, summarized in James et al. (2023a), in which all decisions regarding LP6 placement are fully explained. As the spectral resolution of the FUV detector is expected to decrease as the spectra are moved off-axis (away from LP1, Sahnow et al. 2013, 2022), this program aimed to confirm how fast the degradation in the spectral resolution occurred with increasing cross-dispersion position on the detector, so that the placement of LP6 (and future LPs) could maximize the spectral resolution and lifetime of COS. Analyses of similar resolution programs at other LPs are presented in Roman-Duval et al, (2013), Roman-Duval et al, (2017), Sonnentrucker et al. (2017), Fox et al. (2018), Kerman et al. (2022) and Dieterich et al. (2023).

2. Observations

Program 16495 executed as three visits, each consisting of three orbits between July 17 and 18 2021. The program was impacted by one failed visit, 01, on June 16 2021 due to an HST safing event, and the observations were repeated three weeks later on July 17 2021 in visit 51. The COS observations are summarized in Table 1. We acquired COS FUV G130M/1222 and G160M/1577 spectra of the star AzV 80, to span as wide a wavelength range as possible $\sim 1050 - 1750$Åof the COS/FUV detector. We used two FP-POS to optimize the S/N whilst keeping overheads, increased due to split-wavecals, at a minimum. Once all FP-POS settings are combined, we aimed to reach a

Table 1. Log of exposures for program ID 16495.

Setting	Detector position	Visit	Exposure Time (s)	Dataset ID
G130M/1222	+7”	51	1300	lej651csq, lej651d0q, lej651dgq, lej651dwq
G160M/1577	+7”	51	2767	lej651d8q, lej651doq
G130M/1222	+9”	02	1300	lej602eaq, lej602eiq, lej602eyq, lej602feq
G160M/1577	+9”	02	2767	lej602eqq, lej602f4q
G130M/1222	+11”	03	1300	lej603irq, lej603j1q, lej603joq, lej603k5q
G160M/1577	+11”	03	2767	lej603jgq, lej603jxq

Table 2. Summary of aperture block positions and POSTARG positions needed to place the target at the correct location on the detector.

Step	XAPER	POSTARG	QESIPARM XSTEPS
LP2 (+3.5”)	0	0”	NA
LP2 (+7.0”)	-74	+3.52”	+74
LP2 (+9.0”)	-116	+5.52”	+116
LP2 (+11.0”)	-158	+7.52”	+158

S/N ~ 40/resel to measure a relative change in the spectral resolution, and unexpected variations in the COS line spread functions (LSFs) $> 15\%$.

Azv80 was used instead of the usual target for resolution programs (Azv75) because the visibility windows of Azv75 were too small, meaning AzV75 was not observable in the timeframe needed. The target AzV80 is a blue supergiant star in the Small Magellanic Cloud with spectral type O7 III. The target was chosen to be as UV-bright as possible yet safe for COS, have existing E140M STIS observations, and have high extinction ($E(B-V) = 0.14$) so that strong interstellar absorption line features would be present at a comparable depth to those in Azv75.

Observations were executed relative to LP2 (the nearest calibrated lifetime position on the detector at the time), therefore special commanding was used to set parameters to the appropriate values for the +7”, +9”, and +11” detector positions, as summarized below.

- The focus was set based on the results of program 16491 (Fischer et al. 2022) using the FOCUS parameter in APT. This value needed to be reset after every OSM move.
- For simplicity, we used the LP2 high voltage (HV) values of 173/175 (A/B) for all exposures, since this did not require adjusting the high voltage. This strategy

is based on several earlier programs (LP4 resolution programs 14842 and 15366), which executed successfully.

- The aperture block position was set to XD=+3.5”, XD=+5.5” and XD=+7.5” relative to LP2 in the cross-dispersion direction using the XAPER instruction. With -21 motor steps per arcsecond, the motor step positions are summarized in Table 2.
- The target position was displaced to center the target at the new aperture location using the POS-TARG optional parameter and the XSTEP QESIPARM, summarized in Table 2.

After two 5.3 second target acquisitions with the BOA (to guard against a late guide star acquisition), a 0.1 second initialization exposure was taken to set the aperture position, HV value, and focus values to LP2 defaults before we moved the aperture and changed the focus values relevant for the +7,”, +9” and +11” positions derived from PID 16491. Due to the light leak through the Flat-Field Calibration Aperture (FCA) above +5.5”, TAGFLASH wavecals were disabled (FLASH=NO, WAVECAL=NO in APT). Each science exposure was bracketed by wavecals at LP2 using the default wavecal parameters. The exposure sequence also provided an important test of how LP6 exposures would operate with split-wavecals.

As a comparison to the COS observations, we utilized an existing STIS E140M spectrum of AV 80 from DR2 of the Ultraviolet Legacy Library of Young Stars as Essential Standards (ULLYSES, Roman-Duval et al. 2020). This spectrum was produced by combining STIS E140M echelle grating spectra of AzV 80 from datasets `o4wr12010` and `o4wr12020` from HST proposal ID 7437.

3. Data Reduction

The data were manually reduced using CalCOS v3.3.11, starting from the raw data files (rawtag.fits), because the observations at their detector positions were not supported by the COS pipeline. ASN files were made manually to correctly associate the science and wavecal exposures. Header keywords were set to those for LP2, since the reference files at that LP already existed, and this was the closest calibrated LP in location to the exposures at the time, meaning that these calibration reference files would be most appropriate. In general, we used the standard calibration switches set to default values to produce calibrated x1dsum files. Default reference files for LP2, including BOXCAR extraction with a modified XTRACTAB, were used. To extract data in the correct regions, we modified the LP2 XTRACTAB reference file, notably the B_SPEC, B_BKG1, and B_BKG2 columns for the 1222 and 1577 PSA rows (FUVA and FUVB). Background regions were placed to avoid heavily gain sagged areas of the detector, areas with light leaks through the BOA/FCA, and the glowing edge regions on segment FUVA. The WCA extraction regions were already correctly set for LP2 and were not modified. We used the LP2 DISPTAB, FLATFILE, and FLUXTAB for

wavelength and flux calibration, since this is the closest calibrated LP2 to the observed detector position. The accuracy of the wavelength and flux calibration was checked against STIS data detailed above. The current geometric correction was deemed adequate since the region up to +11" is covered by the GEOFILE reference file.

The S/N of the combined spectrum varies from 15–25 per pixel, corresponding to a S/N of 40–60 per resel across the wavelength range.

4. Analysis

We measured the spectral resolution following previous programs (e.g. Fox et al. 2018), by convolving the much higher resolution STIS E140M spectrum ($R \sim 45000$) of Av80 with a model of the COS LSF for a range of $\pm 50\%$ of the Full-Width at Half Maxima (FWHMs) of the dispersion coefficient. Small shifts in wavelength between the COS and STIS spectra were removed via a cross-correlation analysis. The convolved STIS spectrum was then compared to the on-orbit COS spectra by analyzing the line profiles of narrow interstellar absorption features, as shown in the Appendix. We then measured the resolution by finding the minimum χ^2 of the model-data fit as a function of FWHM. The resolution is characterized as an average over individual resolution measurements from all spectral windows, weighted by the quality of the absorption line feature, where flag=1 is the highest quality, and flag=3 is the lowest quality. This was done separately for each cenwave and segment, using the co-added spectra in the x1dsum files. One spectral window centered on 1153Å was excluded from the analysis due to poor quality fits between the model and the data.

The model LSFs were created using the raytrace models at the +7", +9" and +11" detector positions. The procedure is similar to that in Kerman et al. (2022), and the details can be found therein. The spectral resolution from the models as a function of wavelength for G130M/1222 and G160M/1577 at +7", +9" and +11" can be found in Figure 4.

5. Results

5.1 Spatial resolution

To examine the change in spatial resolution, in Figure 1 we compare the observed cross-dispersion profiles at +7", +9", and +11", for G130M/1222 and G160M/1577. The profiles were created by summing the corrtag images for each individual FP-POS exposure in the cross-dispersion direction and then adding the individual exposures together. The profiles for +7" and +9" are similar, with the +11" profiles being wider at the highest detector position above LP1, as can be seen in the increasing flux in the wings, and the flattening of the peak of the profiles. This shows that spatial resolution degrades with increasing detector position.

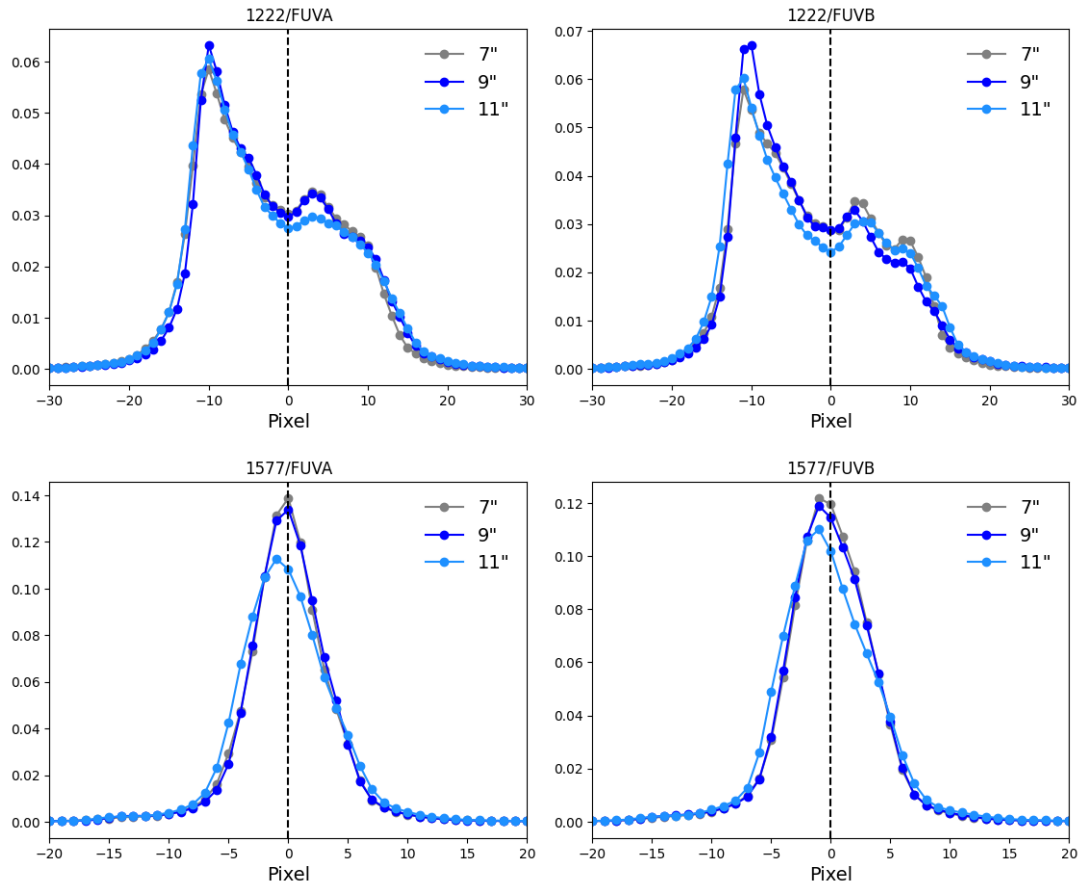

Figure 1. Comparison of the cross-dispersion profiles for G130M/1222 and G160M/1577 at +7", +9" and +11" above LP1. Each profile is the sum of each individual FP-POS exposure. The area under each profile is normalized to 1.

5.2 Spectral resolution

In Figure 2 we show two wavelength regions at all three cross-dispersion positions. By visual inspection the lines are marginally sharper at 7" compared to 11", showing that the spectral resolution decreases with increasing off-axis detector position.

The spectral resolution is measured as $R = \lambda/\Delta\lambda$, where λ is the wavelength, and $\Delta\lambda$ is the FWHM of the best-fit LSF. The spectral resolution at +7", +9" and +11" is summarized as a function of wavelength in Figure 3. The spectral resolution shows a steady decrease from $R \sim 9000-13000$ at +7" to $R \sim 7000-10000$ at +11", where the given range in R encompasses the variation from each cenwave and segment. In general the spectral resolution at +7" is on average $\sim 20-30\%$ lower than that at LP2, where the range includes whether or not 1222A is included, which has a better resolution at +7" than at LP2, and is on average $\sim 20-23\%$ lower than the resolution at LP4. At +9" the spectral resolution is on average $\sim 26-38\%$ ($\sim 26-31\%$) lower than that

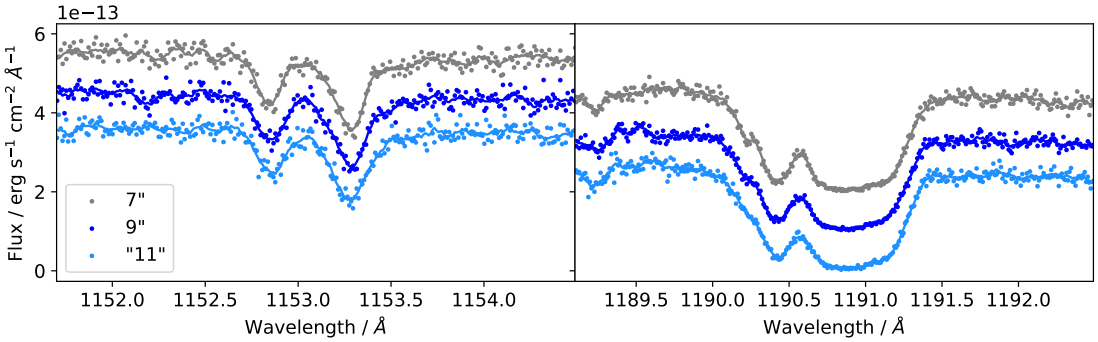

Figure 2. Two wavelength regions at all three cross-dispersion positions for the G130M/1222 spectra. Overplotted is each spectrum boxcar smoothed by 7 pixels to highlight the difference in resolution between detector positions. Spectra are offset from each other in the y-direction for display purposes.

at LP2 (LP4), respectively. At +11" the spectral resolution is on average $\sim 39 - 47\%$ ($\sim 39 - 41\%$) lower than that at LP2 (LP4). Our resolution measurements at +7" are in good agreement with those at LP6 at +6.5" from Kerman et al. (2023).

The same trends are seen with the raytrace models in Figure 4. In general, the model resolution decreases with increasing height on the detector for both G130M/1222 and G160M/1577. The resolution as a function of wavelength changes from a peaked distribution for 1222 at LP2 and LP4 to a more continuously rising distribution with wavelength, which may be related to changes in the PSF with increasing off-axis position. The measured resolution matches the models well, as shown in Figure 5.

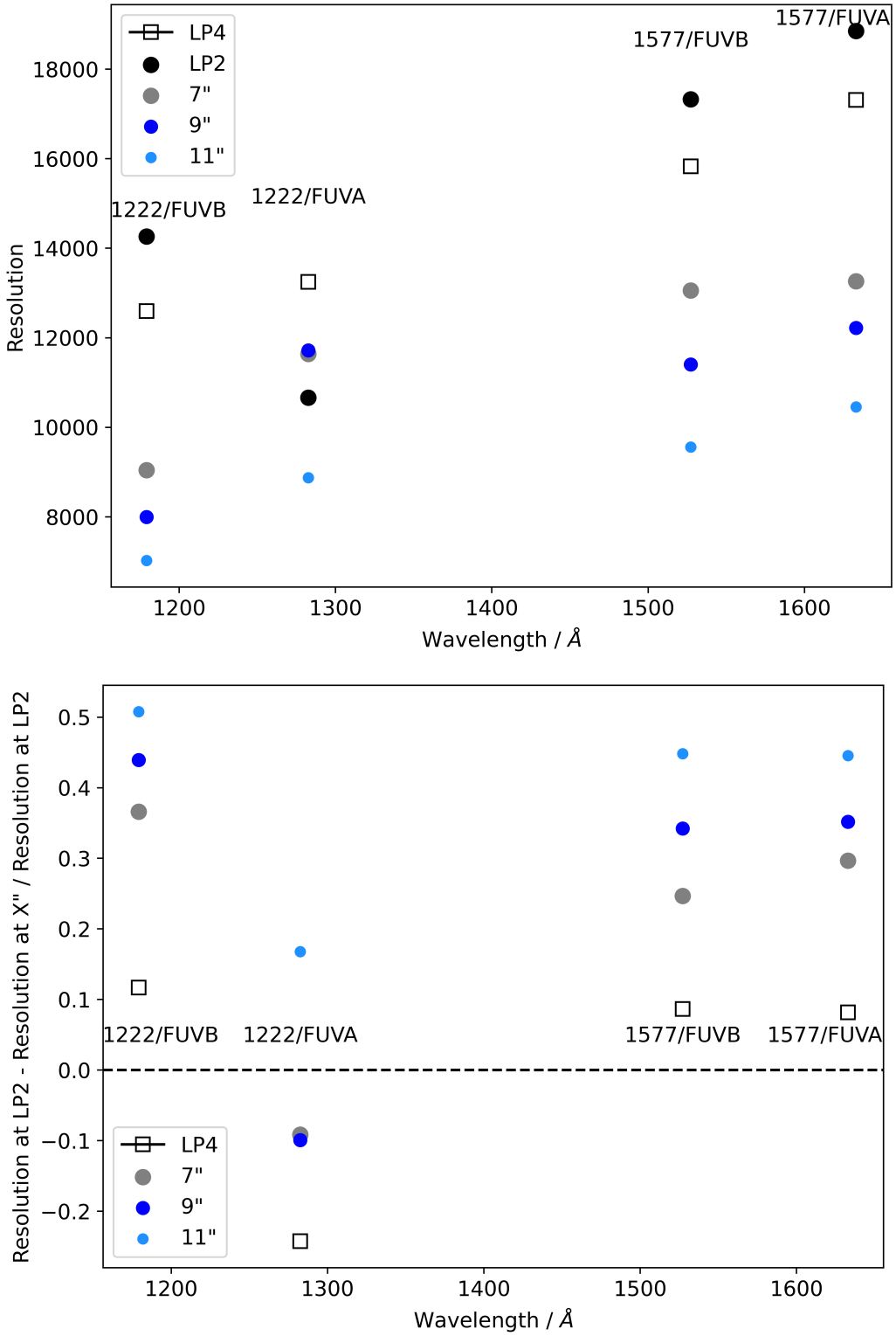

Figure 3. Top: Measured spectral resolution at +7”, +9” and +11” of cenwaves G130M/1222 and G160M/1577 compared to other LPs. Bottom: The difference in the measured spectral resolution at 7”, 9” and 11” compared to LP2, the closest calibrated LP on the detector at the time of the LP6 exploratory program.

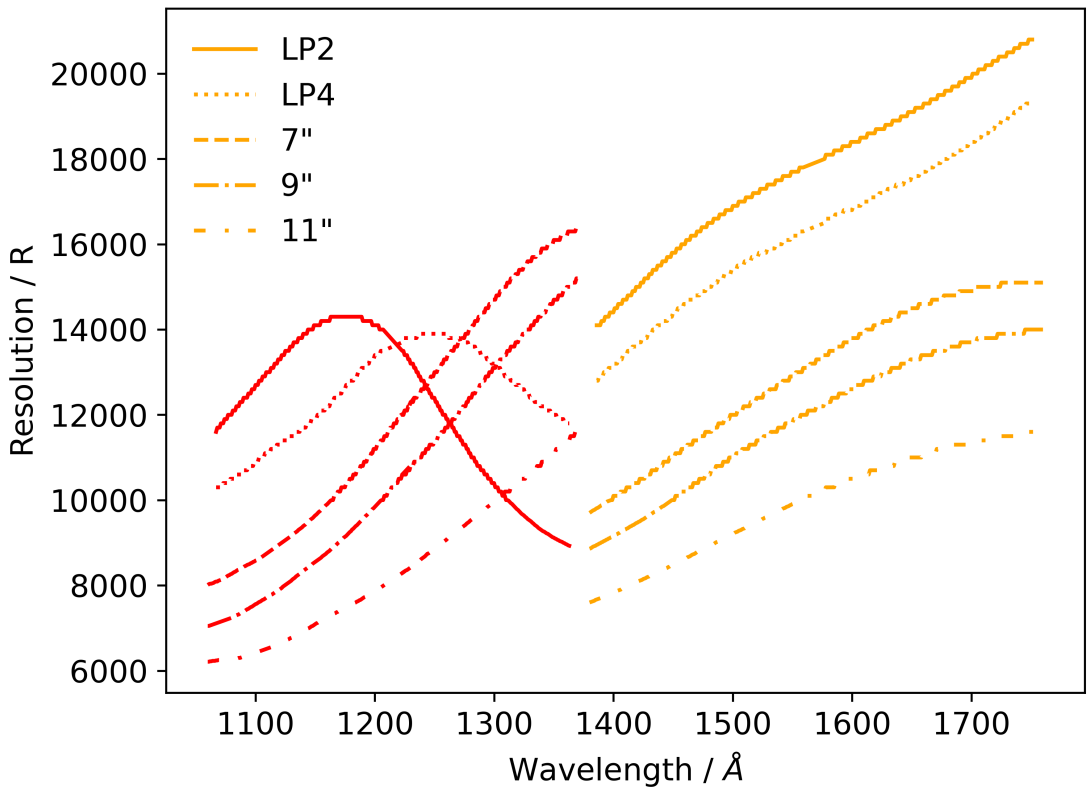

Figure 4. Predicted spectral resolution of the optical models for G130M/1222 (red) and G160M/1577 (yellow) as a function of wavelength at +7”, +9” and +11”, compared to other LPs.

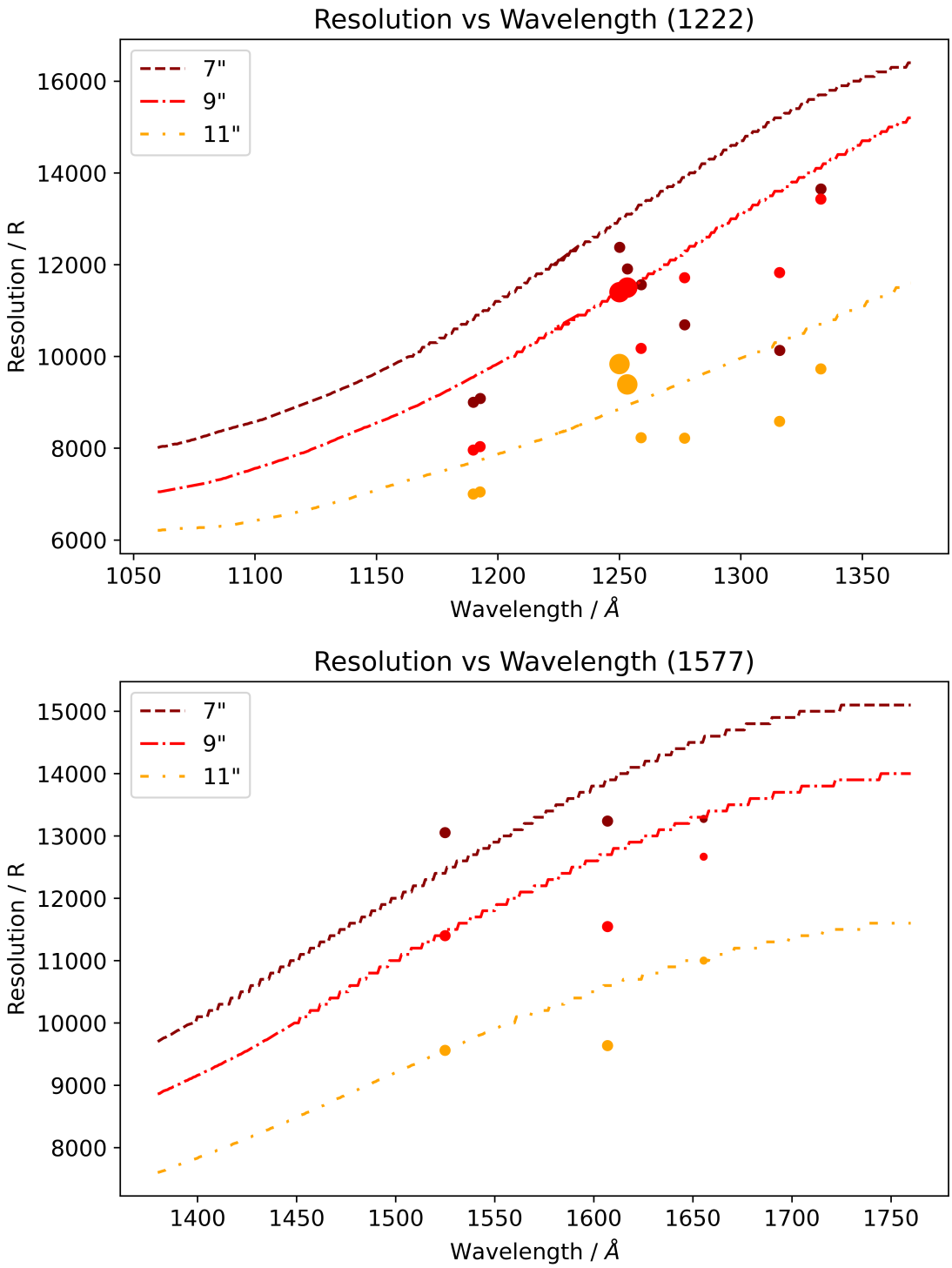

Figure 5. Measured and predicted spectral resolution of the optical models for G130M/1222 (top) and G160M/1577 (bottom) as a function of wavelength at +7", +9" and +11". The size of the points indicated the quality of the spectral window, with larger points indicating higher quality, which are given more weight in the overall resolution calculation for each cenwave.

6. Conclusions

We investigated the spectral resolution of the COS detector from +7 to +11" above LP1, to inform the placement of future lifetime positions, including LP6. Using data and models we found that the spectral resolution shows a steady decrease from $R \sim 9000 - 13000$ at +7" to $R \sim 7000 - 10000$ at +11". In general the spectral resolution at +7" is 20–30% lower than that at LP2 and LP4. The decrease in resolution with increasing detector position motivated placing LP6 as low on the detector as possible, to maintain the highest possible resolution at LP6, to subsequently optimize the amount of future high spectral resolution science with COS. LP6 was placed at +6.5" above LP1 on the detector, and G130M/1222 remained at LP4. These spectral resolution measurements provide a valuable dataset for optimizing the placement of future lifetime positions and extending the lifetime of COS beyond 2030.

Acknowledgments

We thank William Januszewski, George Chapman and Merle Reinhart for their efforts in scheduling this program, and Olivia Lupie, Scott Swain, Mike Kelly and Beverly Johnson from Goddard Space Flight Center for their support of this complex program.

Change History for COS ISR 2024-05

Version 1: 28 March 2024- Original Document

References

Dieterich et al., 2023, COS Instrument Science Report 2023-08
Fischer et al., 2022, COS Instrument Science Report 2022-12
Fox et al., 2018, COS Instrument Science Report 2018-07
James et al. 2023a, COS Instrument Science Report 2023-15
Kerman et al. 2023, COS Instrument Science Report 2023-02
Roman-Duval, et al., 2013, Instrument Science Report COS 2013-07
Roman-Duval, et al., 2017, COS Instrument Science Report 2017-06
Sahnow, et al., 2013, COS Instrument Science Report 2013-13
Sahnow, 2022, Proceedings of the SPIE, Volume 12181, 1218136
Sonnentrucker et al., 2017a, COS Instrument Science Report 2017-16
Sonnentrucker et al., 2017b, COS Instrument Science Report 2017-20

Appendix A

Here we plot comparisons of the COS data with a grid of models at different resolution for for different wavelength regions, at +7", +9" and +11".

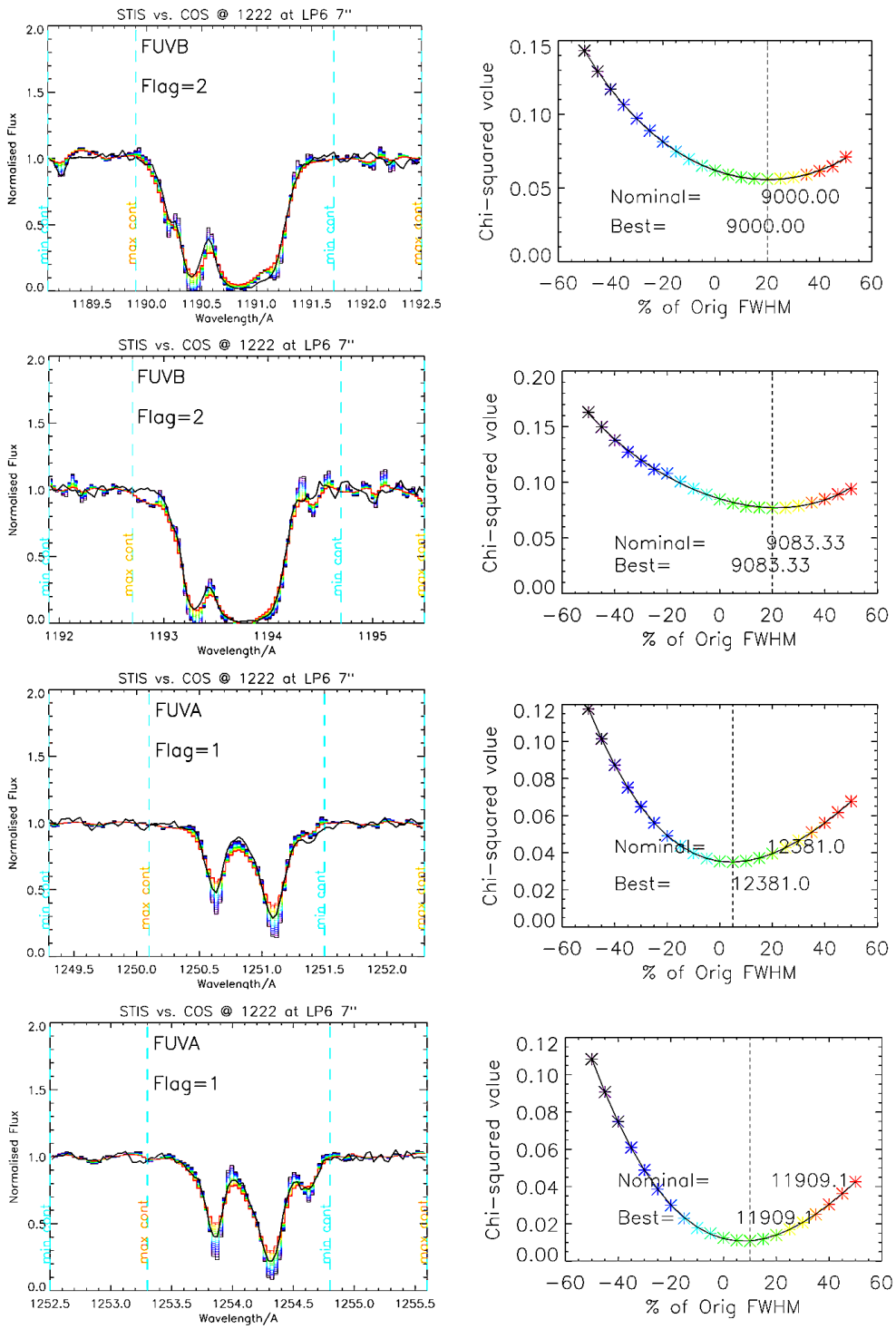

Figure 6. Left: Comparison of G130M/1222 COS data at +7" (black) with a grid of models at different resolution (solid colored curves) for different wavelength regions. The dashed blue lines indicate the continuum normalization windows. Right: The distribution of χ^2 vs % of modeled FWHM. Zero corresponds to the nominal FWHM value at +7", with the best-fitting value denoted by the dashed vertical line.

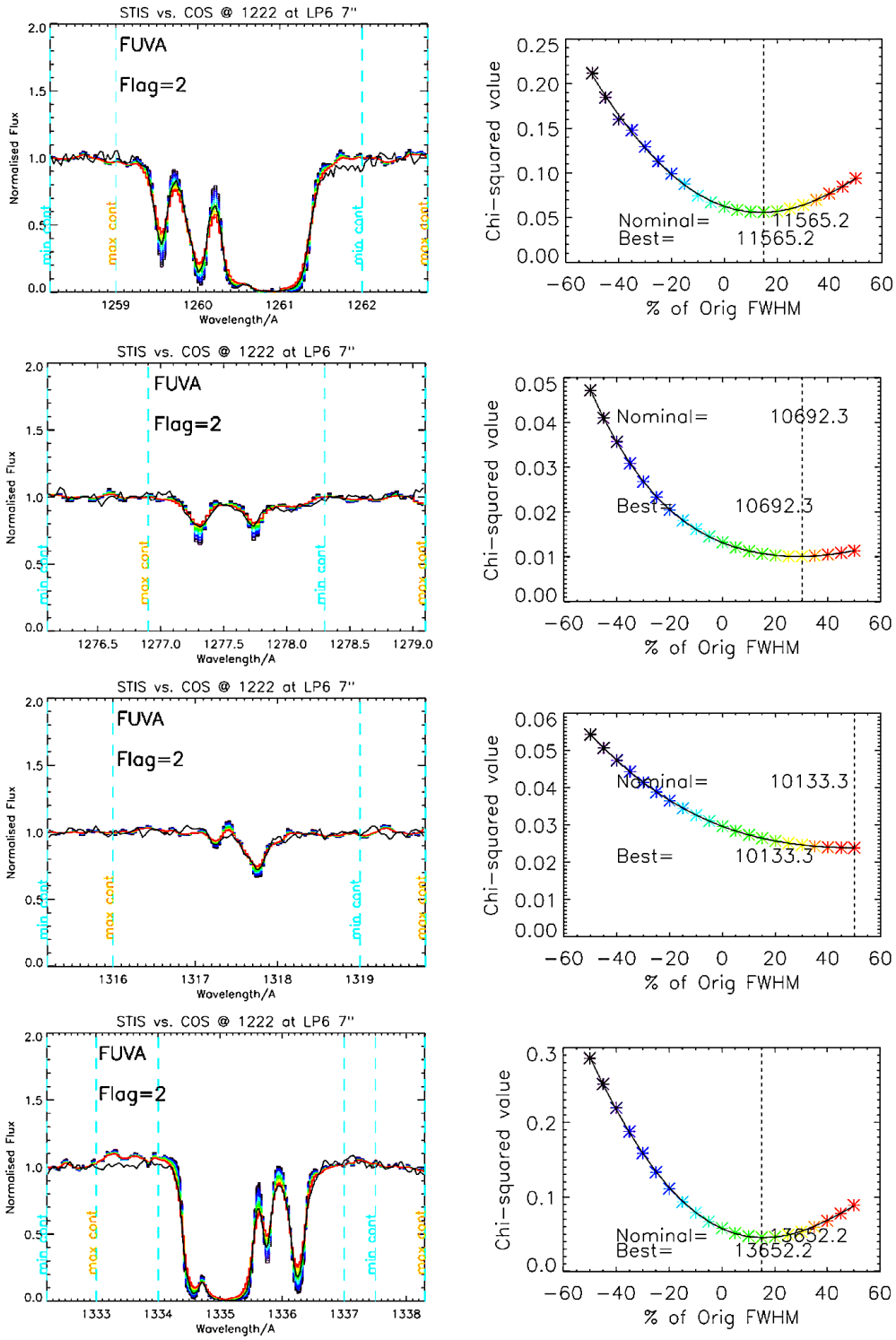

Figure 7. Same as Figure 6.

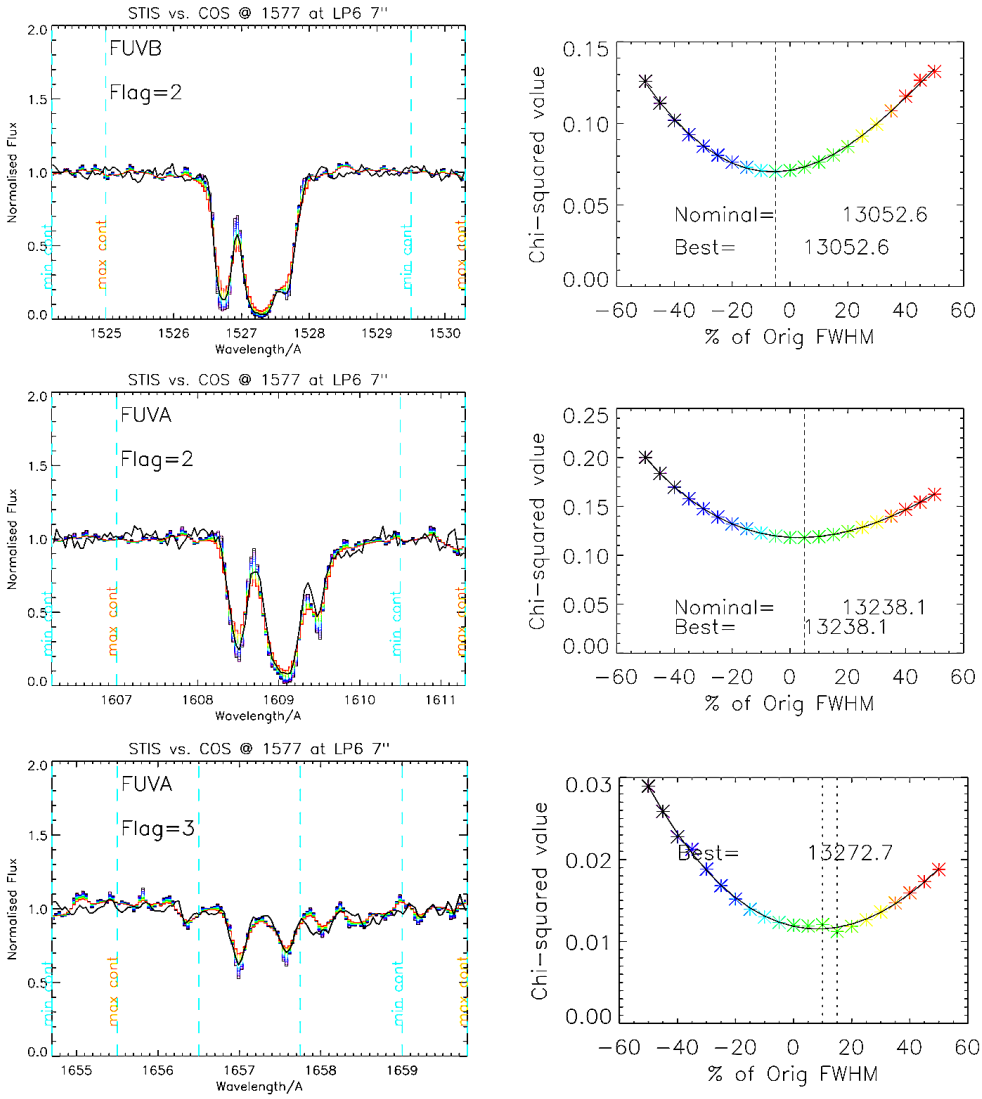

Figure 8. Same as the Figure 7 but for G160M/1577 at +7".

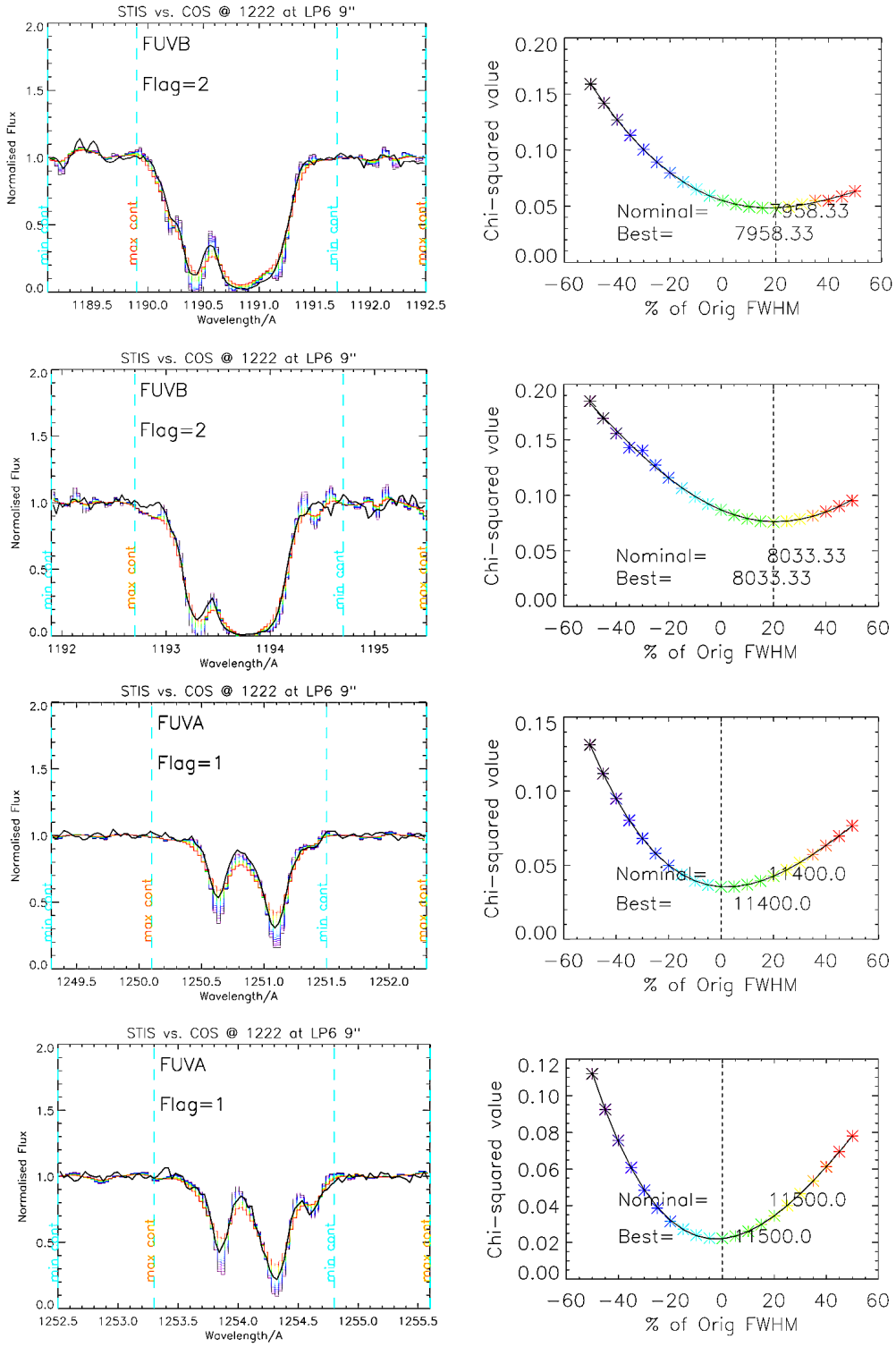

Figure 9. Left: Comparison of G130M/1222 COS data at +9" (black) with a grid of models at different resolution (solid colored curves) for different wavelength regions. The dashed blue line indicates the continuum normalization windows. Right: The distribution of χ^2 vs % of modeled FWHM. Zero corresponds to the nominal FWHM value at +9", with the best-fitting value denoted by the dashed vertical line.

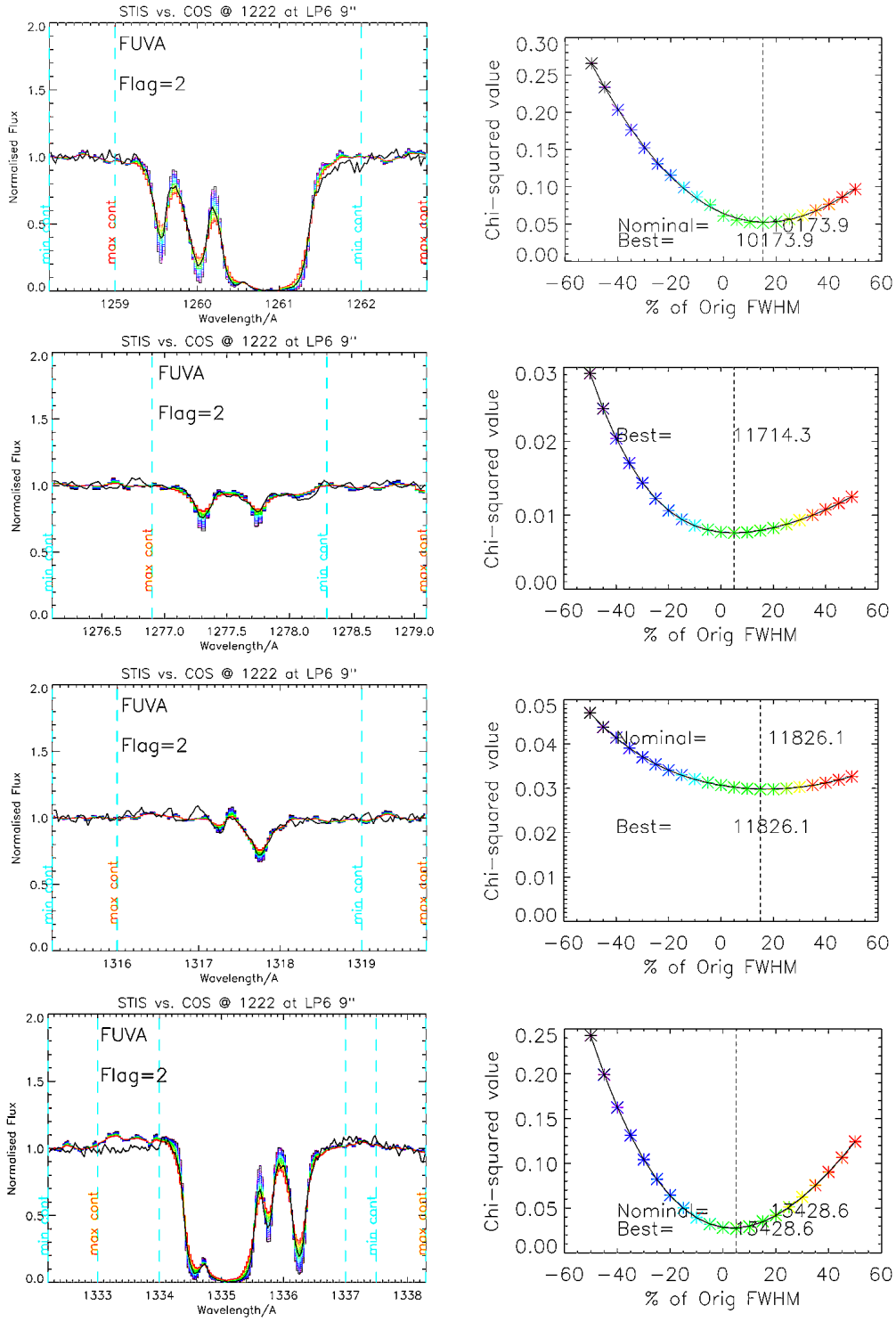

Figure 10. Same as Figure 9.

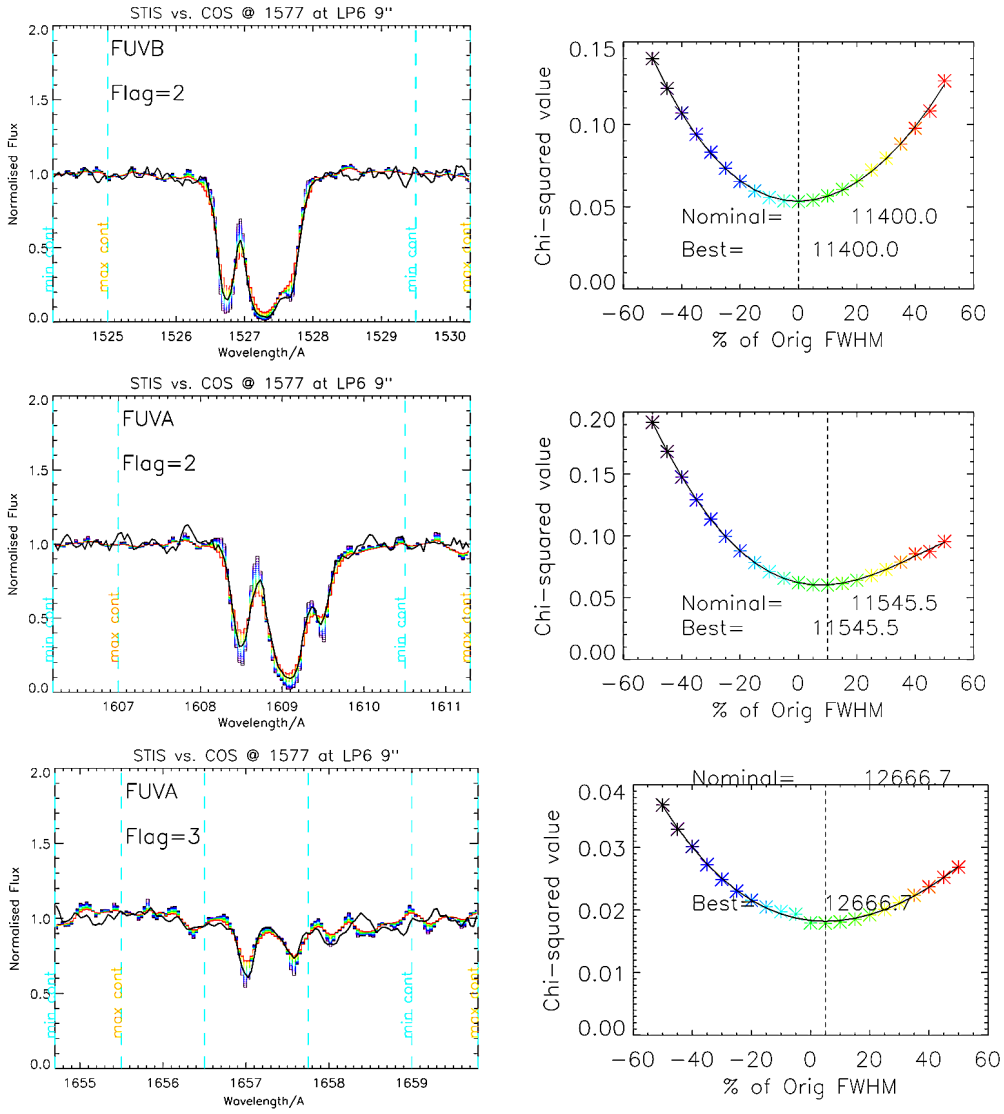

Figure 11. Same as Figure 10 but for G160M/1577 at +9".

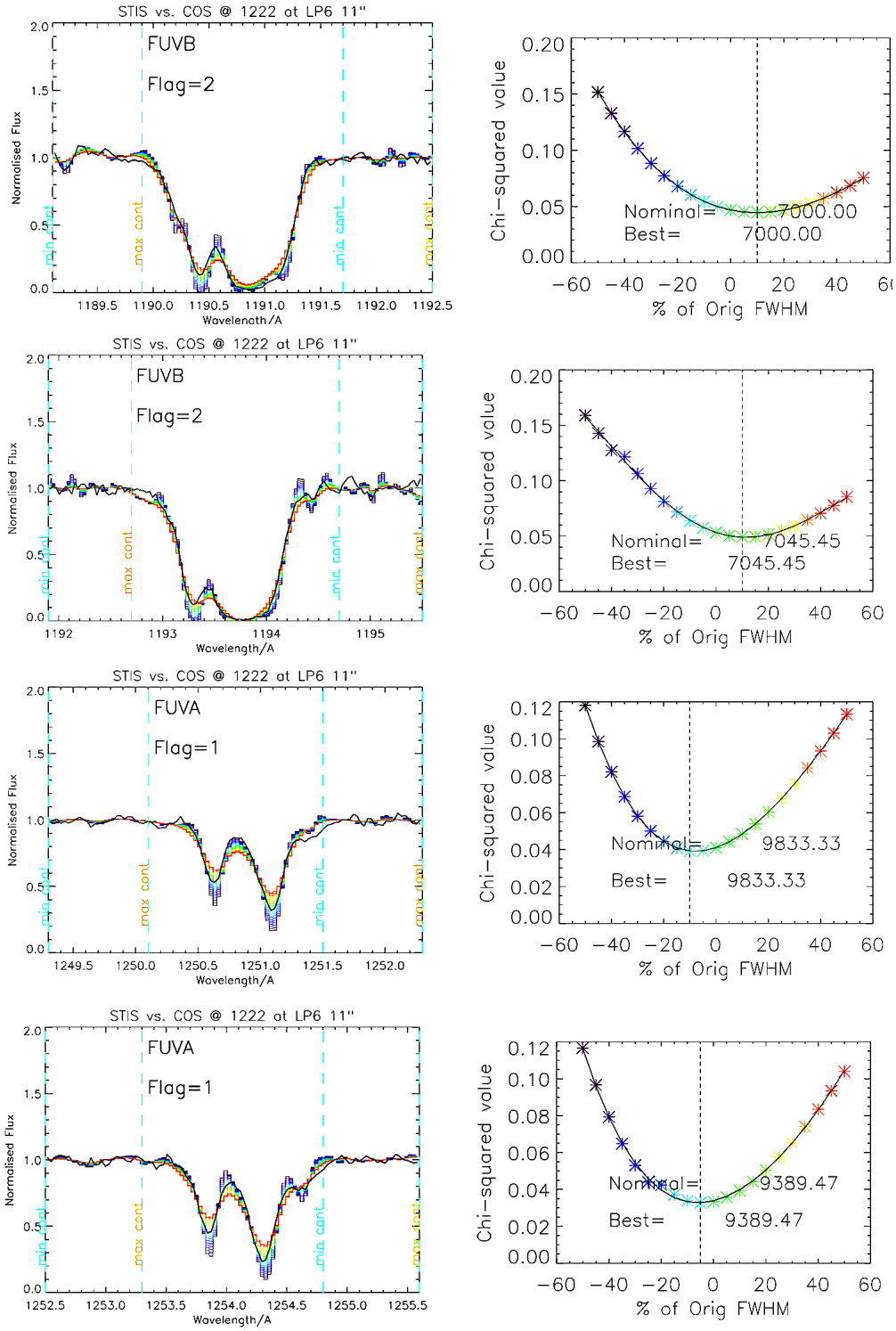

Figure 12. Left: Comparison of G130M/1222 COS data at +11" (black) with a grid of models at different resolution (solid colored curves) for different wavelength regions. The dashed blue line indicates the continuum normalization windows. Right: The distribution of χ^2 vs % of modeled FWHM. Zero corresponds to the nominal FWHM value at +11", with the best-fitting value denoted by the dashed vertical line.

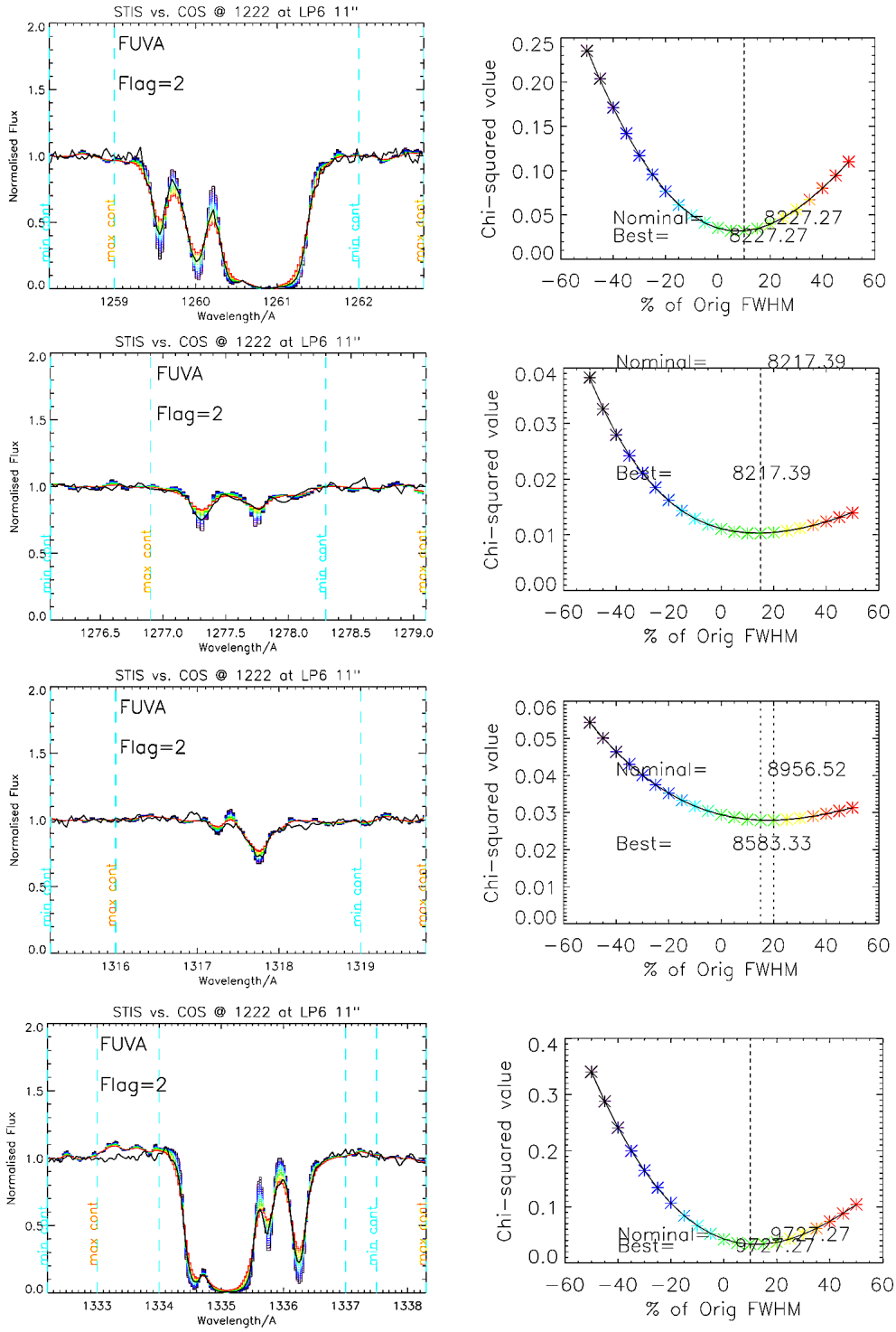

Figure 13. Same as Figure 12.

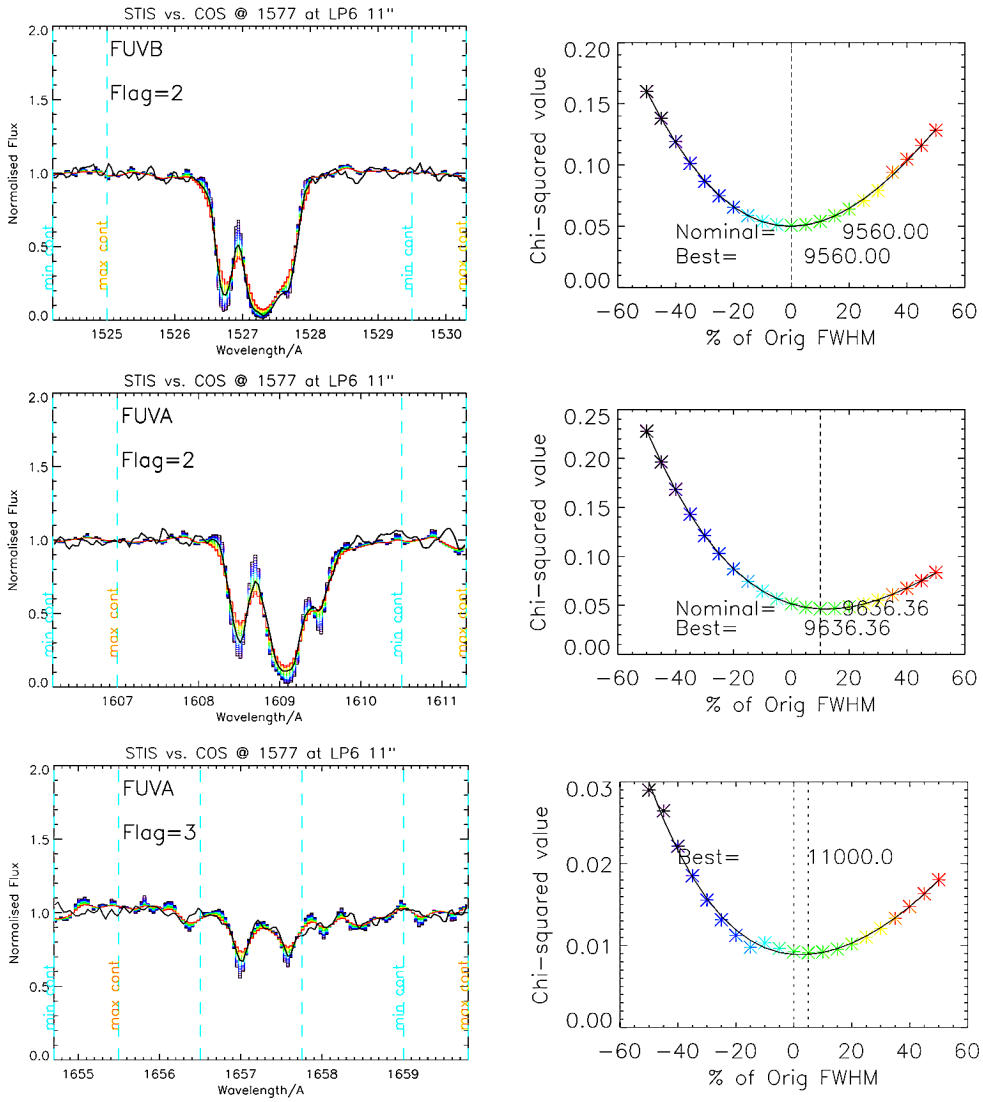

Figure 14. Same as Figure 13 but for G160M/1577 at +11".